Hydrogel Microcapsules with Photocatalytic Nanoparticles for Removal of Organic Pollutants

SCHOLARONE™
Manuscripts

1
2
3
4
5
6
7
8
9
10
11
12
13
14
15
16
17
18
19
20
21
22
23
24
25
26
27
28
29
30
31
32
33
34
35
36
37
38
39
40
41
42
43
44
45
46
47
48
49
50
51
52
53
54
55
56
57
58
59
60

Glass capillary-based microfluidic technique enables a highly efficient encapsulation of photocatalytic nanoparticles in thin shell hydrogel microcapsules. Poly(methacrylic acid)-derived hydrogel membranes can be used to carry, separate and release molecular species, particulates and reaction products reversibly and selectively. Encapsulation of photocalytic TiO_2, ZnO nanoparticles in the hydrogel capsules for the removal of MB from aqueous solutions is demonstrated using adsorption and oxidation mechanisms. Microcapsules with the photocatalytic liquid core lead to a removal of MB organics, while the flow microreactor device is demonstrated to reduce time of water cleaning.

ARTICLE

Hydrogel Microcapsules with Photocatalytic Nanoparticles for Removal of Organic Pollutants

Jinrun Liu,[a] Hong Chen,[a] Xiaojie Shi,[a] Saraf Nawar,[b] Jörg G. Werner,[b] Gaoshan Huang,[a] Miaomiao Ye,[c] David A. Weitz[b‡] Alexander A. Solovev*[a] and Yongfeng Mei*[a]

Droplet-based microfluidics is used to fabricate thin shell hydrogel microcapsules for the removal of methylene blue (MB) from aqueous solutions. The microcapsules composed of a poly(methacrylic acid) hydrogel shell exhibit unique properties, including permeation, separation, purification, and reaction of molecular species. Photocatalytic TiO_2 and ZnO nanoparticles encapsulated in the microcapsules, i.e. photocatalyst in capsule (PIC), are used to remove organic pollutants using an adsorption-oxidation mechanism. A prototype flow microreactor is assembled to demonstrate a controllable water purification approach in short time using photocatalysts. Our studies of aqueous and homogeneous hydrogel environments for the photocatalysts provide important insights into understanding the effectiveness of MB removal. Hydrogel capsules have MB removal rate comparable to homogeneous particles. Further reduction of both capsule and photocatalyst sizes can potentially aid in quicker water purification.

Environmental significance

Glass capillary-based microfluidic technique enables a highly efficient encapsulation of photocatalytic nanoparticles in thin shell hydrogel microcapsules. Poly(methacrylic acid)-derived hydrogel membranes can be used to carry, separate and release molecular species, particulates and reaction products reversibly and selectively. Encapsulation of photocalytic TiO_2, ZnO nanoparticles in the hydrogel capsules for the removal of MB from aqueous solutions is demonstrated using adsorption and oxidation mechanisms. Microcapsules with the photocatalytic liquid core lead to a removal of MB organics, while the flow microreactor device is demonstrated to reduce time of water cleaning.

Introduction

The various mechanisms of pollutant removal involve separation, adsorption, desorption, oxidation and degradation.[1] Typical adsorbents include gypsum, activated carbon, chitosan, fly ash, zeolite, clay minerals, peat and wood.[2] Application of nanomaterials, such as carbon nanotubes, microspheres and flowerlike ferric hydroxide[3] increases the surface area (higher adsorption capacity) of adsorbents. Moreover, additional catalytic materials can be included to degrade hazardous organics using released radical species (OH·, HOO·, or $O_2 \cdot^-$) to accomplish cleaning via an adsorption-oxidation-desorption mechanism.[4] For instance, the maximum adsorption capacity of

465.5 mg g^{-1} was reported for methylene blue using gelatin, iron oxide nanoparticles and carbon nanotube nanocomposites.[5] Using photocatalysts, such as TiO_2, ZnO, Fe_2O_3, WO_3, Ag_2CO_3, ZnS and $BiTiO_3$, it is feasible to generate OH· using solar light without additional chemicals. [6, 7] Photocatalysts offer highly efficient and environmentally friendly routes to decompose undesired contaminants in water. Wide band gap semiconductors (e.g. TiO_2, ZnO) utilize solar light to achieve oxidation and provide a promising green technology for water purification.[8, 9] Upon illumination of semiconductors, electron-hole pairs are created. Holes react with water to form hydroxy radicals, while electrons react with oxygen to form superoxide anion. [10-12] However, bulk semiconductors suffer from low surface area and thus, a significantly lower number of catalytic sites are available. A high surface area of adsorbent/catalyst helps to capture a large amount of pollutants and reduce the amount of expensive adsorbents/catalysts.[13] On the other hand, nanoparticles dispersed in rivers and lakes represent an environmental contamination themselves. Hence, it is highly desirable to encapsulate NPs in three-dimensional matrices, e.g. graphene supported catalysts for organic dyes degradation.[14]

Hydrogels can absorb a large quantity of water and retain it without dissolution for applications including forward osmosis, desalination, wastewater clean-up, removal of microbial, chemical and biohazardous threats.[15] Hydrogels can swell or deswell in response to changes in pH, solvent composition, magnetic, electric fields and ultrasound irradiation. Permeability of hydrogel films can be controlled, for example, by tuning the composition ratio between polyethylene glycol diacrylate (PEGDA) and RNH_3Cl monomers.[16] Water purifying materials can be physically entrapped in hydrogel network for adsorption, separation and removal of dyes and heavy metal

a. Department of Materials Science, Fudan University, 220 Handan Road, Shanghai 200433, People's Republic of China; solovevlab@gmail.com; yfm@fudan.edu.cn
b. John A. Paulson School of Engineering and Applied Sciences and ‡Department of Physics, Harvard University, Cambridge, MA 02138, USA
c. Zhejiang Key Laboratory of Drinking Water Safety and Distribution Technology, College of Civil Engineering and Architecture, Zhejiang University, Hangzhou,310058, People's Republic of China

ARTICLE   *Environmental Science: Nano*

ions.[17] Hybrid nanoparticle-hydrogel composites linked via physical adsorption or covalent bonds enable highly efficient adsorptive removal of aqueous pollutants.[18-22] Recently polymer nanocomposites were shown to have a high potential to avoid agglomeration of high surface area nanoparticles for water cleaning operations.[23] Other examples include, graphene oxide-based hydrogel particles are demonstrated for oil decontamination.[24] Hydrogels embedded with hydrated Ferric Oxide nanoparticles are used for arsenate removal.[25] A tripeptide-based hydrogel is shown for removal of toxic organic dyes and lead (Pb^{2+}) ions,[26] and laccase immobilized hydrogel are designed for removal of Bisphenol A.[27] In addition, hydrated polymer networks and nanostructured hierarchical membranes can be prepared for water purification using solar-induced vapourization.[28, 29] For instance, ionisable aromatic pollutants are removed from water using nano gamma-Fe_2O_3 containing cationic hydrogel.[30] Moreover, water desalination using hydrogel membranes for obtaining solar-induced vapourization[31] and using forward osmosis[32] have recently attracted high attention.[33] Graphene-based hydrogels with agarose (AG) as a stabilizer, reducing agent and the polydopamine functionalized graphene hydrogels (PDA-GH) are shown to enhance degradation and removal of toxic dye pollutants, organic solvents, heavy metal ions (Cd^{2+}, Pb^{2+}, Cu^{2+}) and oils.[34] Certain challenging aspects of hydrogel filtration must be taken into account, such as embedded composite adsorbents/catalysts, adsorption kinetics, operations in wider pH ranges, time of filtration, regeneration, reusability and resources recovery.[35]

Recently, the development of environmental micromotors powered by external magnetic fields,[36, 37] as well as light-driven (photocatalytic, plasmonic)[38-42] and chemical fuel powered catalytic/hybrid (i.e., H_2O_2) micromachines has attracted attention.[43-51] Particularly, micromotors are capable to outswim diffusion,[52] generate reactive species, and, as a result, lead to more efficient decontamination of pollutants in shorter times.[53, 54] Various active materials, including carbon/MnO_2[55] metal oxides[56] hydrogel/emulsion-hydrogel[57] MOF-based[58] catalytic DNA-functionalized[59] carbon[60] graphene[61] MnO_2, Ag[62] silver-exchanged zeolite[63] magnesium[64] have been demonstrated. Organic pollutants can undergo degradation assisted by H_2O_2, $NaBH_4$, photocatalytic or biocatalytic processes.[65] For instance, methylene blue (MB) has been successfully removed using layered manganese oxide micromotors in H_2O_2 solutions.[66]

Herein, we report a water cleaning architecture employing encapsulated photocatalytic nanoparticles in poly(acid) hydrogel microcapsules. The microcapsules are fabricated using complex water-in-oil-in-water double emulsion drops produced from a glass capillary microfluidic devices. An aqueous dispersion of photocatalytic nanoparticles and methacrylic anhydride form the core and shell of the double emulsion drops, respectively. Upon photo-polymerization and hydrolysis, poly(methacrylic acid) hydrogel microcapsules containing photocatalytic nanoparticles in the aqueous core are obtained. Microcapsule shells exhibit reversible pH-responsive permeability,[68] and the dynamic capsules self-propel in

hydrogen peroxide solutions.[69] Thin shell hydrogel microcapsules with a photocatalytic aqueous core can potentially provide enhanced reaction, diffusion, and separation of molecular species in comparison to bulk hydrogels with embedded nanoparticles.[70] Dynamic properties of microcapsules (magnetic, self-propelled) and a prototype flow
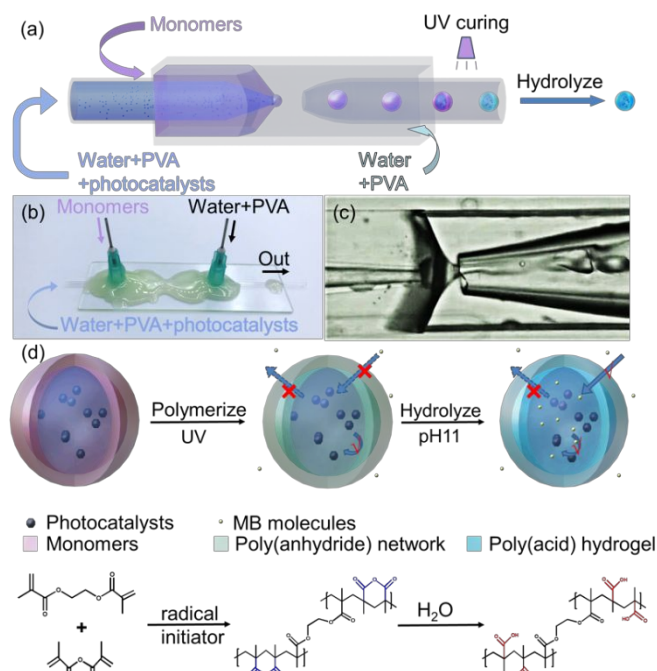
reactor device with a layer of microcapsules are demonstrated to reduce time required for MB removal.

Figure 1. Fabrication of hydrogel microcapsules with aqueous core containing photocatalytic nanoparticles. Schematic illustration (a), optical image (b), and optical microscopy image (c) of the capsules generation using glass capillary microfluidic device; (d) photo-polymerization of methacrylic anhydride and ethylene glycol dimethacrylate leads to a poly(anhydride) network in the shell that hydrolyses to form poly(acid) hydrogel microcapsules.

2. Results and discussion

2.1 Fabrication and characterization of microcapsules

A glass capillary microfluidic device is used to produce monodisperse double emulsion microdrops with the desired diameter, shell thickness and aqueous core.[67, 68] **Figure 1a** shows the experimental setup: two tapered cylindrical capillaries aligned inside a slightly larger square capillary. Methacrylic anhydride (MAAn), ethylene glycol dimethacrylate (EGDMA) are used as monomers and oil to fabricate the double emulsion drops with added radical photoinitiator 2-hydroxyl-2-methylpropiophenone (Darocure 1173). MAAn is water immiscible, leading to the formation of an acid-precursor-containing shell around a hydrophilic aqueous core. When hydrolysed to poly(methacrylic acid), the EGDMA cross-linker

retains the structural integrity of the capsules. As shown in **Figure 1a**-**c**, the outer phase (water + PVA), the inner phase (water + PVA + photocatalysts), and the middle phase (monomers) are used to assemble monodisperse double emulsion drops containing photocatalysts in the core. As illustrated in **Figure 1d**, exposure to UV light leads to photo-polymerization of the hydrophobic poly(anhydride) networks.[68] After treating the microcapsules in pH11 for 24 hours, the anhydride groups (red colour, **Fig. 1d**) of the poly(anhydride) network are cleaved to carboxylic acid groups (blue colour), which results in a hydrophilic poly(acid) network.
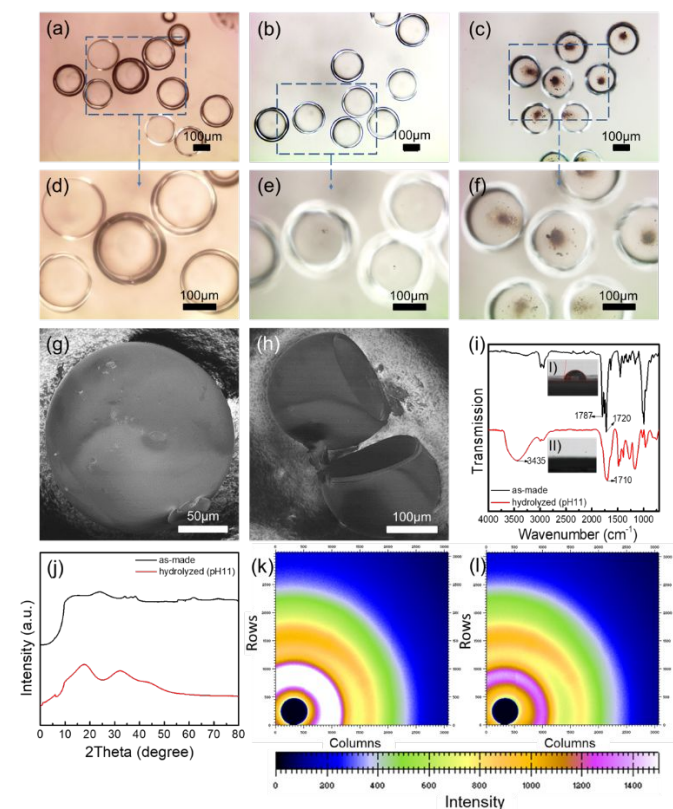

Figure 2. Optical microscopy (a-f), SEM images (g, h), and FTIR results (i) of the prepared microcapsules, ZnO in capsules, and TiO_2 in capsules. Corresponding contact angles of poly(anhydride) network: inset images (i: I) and poly(acid) hydrogel (i: II). (j) X-ray diffraction patterns and 2D wide-angle scattering profiles (k, l) of the hydrophobic poly (anhydride) network and the poly (metharylic acid) hydrogel, respectively.

Figure 2a-**h** illustrates optical microscopy and FESEM images of fabricated hydrogel capsules showing a visible aggregation of nanoparticles in the aqueous core. **Figure 2b-f** shows the ZnO (**Figure 2b**, **e**) and TiO_2 (**Figure 2c**, **f**) nanoparticles in capsules. **Figure 2g**, **h** shows the FESEM images of a single capsule and a collapsed capsule (diameter ~200μm, shell thickness 5 μm), respectively. SEM images of TiO_2 nanoparticles, ZnO nanoparticles, TiO_2 nanoparticles in microcapsule, ZnO

nanoparticles in microcapsule, and the corresponding elemental mapping images of element C, O, Ti, and Zn are shown in **Figure S3**. The photocatalysts' particle sizes were measured by laser particle analyzer (Nano ZS90, Malvern, UK), the results are shown in **Figure S4.** Analysis of particle size distribution indicates that an average size of TiO_2 and ZnO nanoparticles are 259 nm and 456 nm, respectively. A Fourier transform infrared spectroscopy (FTIR) is used to confirm the hydrolysis of the capsules, shown in **Figure 2i**. We see the presence of an absorption band around 3000-3500 cm^{-1}, corresponding to O-H stretching, which is typically observed only in the FT-IR spectrum of hydrolysed capsules. In addition, the contact angle is measured to study the wettability of the surfaces of the poly(anhydride) network and the poly(acid) hydrogel, shown in the inset **Figure 2i (I)** and **Figure 2i (II)**. The measured contact angle of the poly(anhydride) network is 83°, indicating that the poly(anhydride) network is hydrophobic, while the contact angle of the poly(acid) hydrogel is close to 0°, proving that the poly(anhydride) network is hydrolyzed to hydrophilic poly(acid) hydrogel. **Figure 2j-l** shows the X-Ray Diffraction (XRD) and 2D Wide Angle X- ray Scattering (WAXS) patterns (**Fig. 2k, l**) of the hydrophobic poly (anhydride) network and poly (metharylic acid) hydrogel. In this measurement, both the poly(anhydride) network and the hydrolyzed poly(acid) hydrogel are amorphous and the broad bands of poly(acid) hydrogel are at 18° and 32° indicating that after hydrolysis the poly(acid) hydrogel gets more ordered than the poly(anhydride) network. Stability in salts was also measured by inserting capsules in 1 M NaCl and 1 M K_2SO_4 aqueous solution for 7 days (Figure S2).

2.2.1 Adsorption and photocatalytic degradation

MB is used as a model organic dye pollutant to estimate the adsorptive performance and photocatalytic oxidation using synthesized capsules. To demonstrate the adsorption and photocatalytic activity, samples are immersed in the MB aqueous solution. **Figure 3a-g** shows the temporal evolution of MB concentrations in aqueous solution in the dark and under UV light. For comparing hydrogel capsules and particles, TiO_2 nanoparticles are mixed with homogeneous hydrogel precursor to form spherical microparticles (HHP) with diameters of ~200 μm (optical and SEM images are shown in **Fig. S1**, Supporting Information). In the latter case, TiO_2 is mixed using the same procedure, followed by an exposure to UV light and 24 hours treatment in pH=11 KOH solution. Microcapsules, TiO_2 in capsules, ZnO in capsules, TiO_2 in particles, bare ZnO nanoparticles, and bare TiO_2 nanoparticles adsorb 83.46%, 91.98%, 89.48%, 93.06%, 16.90%, 13.83% of the MB, respectively. A new equilibrium is established in ~40 min due to adsorption of MB in hydrogels, shown in **Figure 3h**. PIC and HHP have enhanced removal rate of MB by adsorption in comparison to bare photocatalysts. With UV light on bare nanocatalyst degrade MB to similar values during one hour. The high adsorption efficiency of the samples is related to the porous structure of hydrogels. After 80 min soaking, UV light was

turned on (**Fig. 3**). During exposure to UV light the photocatalytic degradation of MB is realized by photo-induced holes (h^+) and their secondary products $\cdot$OH, $HO_2\cdot$. A new equilibrium is established due to consumption of MB in microcapsules, where more MB molecules are absorbed in the solution and the MB concentration decreases further, shown in **Figure 3h**. A negligible change due to photodegradation is observed in the aqueous solution using MB (w/o microcapsules) and bare microcapsules (w/o photocatalyst), while ZnO and TiO_2 in capsules removed nearly 100% of the MB in aqueous solutions. PIC shows a photocatalytic removal of MB comparable to HHP (3.61% of the original MB concentration remained in HPP). Recently reported non-equilibrium uptake kinetics simulation results[70-74] indicate that hydrogels' polymer chains can restrict solute dynamics, and the mobility of co-solutes can be reduced due to specific adsorption. In agreement with this explanation, we detected that PIC have a slightly enhanced photocatalytic performance than

TiO_2 in homogeneous particles. Both PIC and TiO_2 in HHP are decoloured upon UV exposure, meanwhile no significant change was detected in an aqueous solution with MB (w/o microcapsules) and bare capsules (w/o photocatalyst), shown in **Figure 5**. PIC and HHP are decolored from the dark blue to the original transparent colour by exposing samples to UV light during 120 min. FTIR measurements were performed to confirm the adsorption and photocatalytic degradation of MB in PIC, as shown in Figure 5. Bands at 1596 cm^{-1} and 1330 cm^{-1} correspond to C=N aromatic and C-N aromatic bonds in MB, respectively, and band at 1247 cm^{-1} is attributed to the C-N aliphatic band in MB. After the adsorption process, the PIC were in blue colour, these bands appeared, indicating the presence of MB. And after UV exposure the PIC gets its original transparent colour, the bands disappeared, it suggests the cleavage of C=N aromatic, C-N aromatic, and C-N aliphatic band because of photocatalytic degradation.
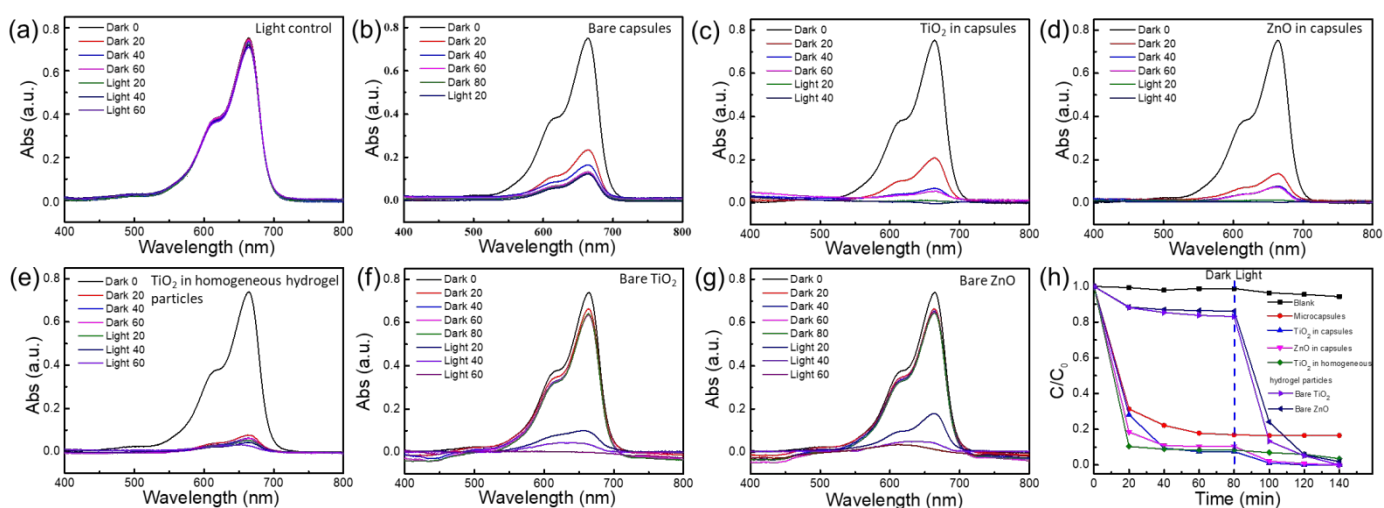

Figure 3. UV-vis absorption spectra of solution with MB and solutions containing both MB and photocatalytic microcapsules under dark and UV light conditions. Legends display time in minutes. (a) Light control experiment. (b) Bare capsules without photocatalyst. (c) TiO_2 in aqueous core of hydrogel capsules. (d) ZnO in aqueous core of hydrogel capsules. (e) TiO_2 in homogeneous hydrogel particles. (f) Bare TiO_2 nanoparticles. (g) Bare ZnO nanoparticles. (h) Removal curves of the samples.
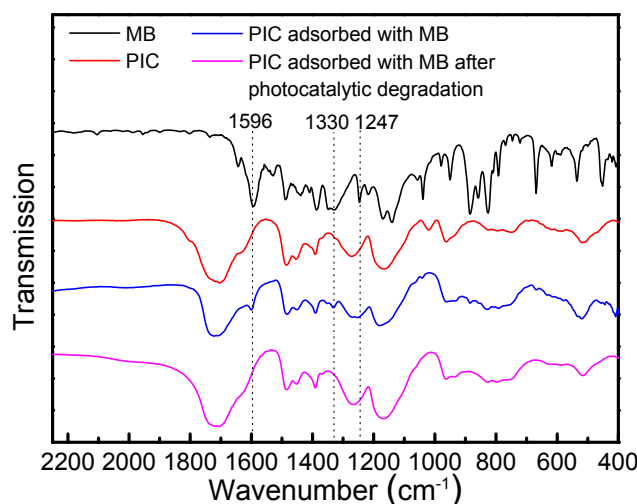
Figure 4. FTIR spectrum of MB, PIC, PIC adsorbed with MB, and PIC adsorbed with MB after photocatalytic degradation.
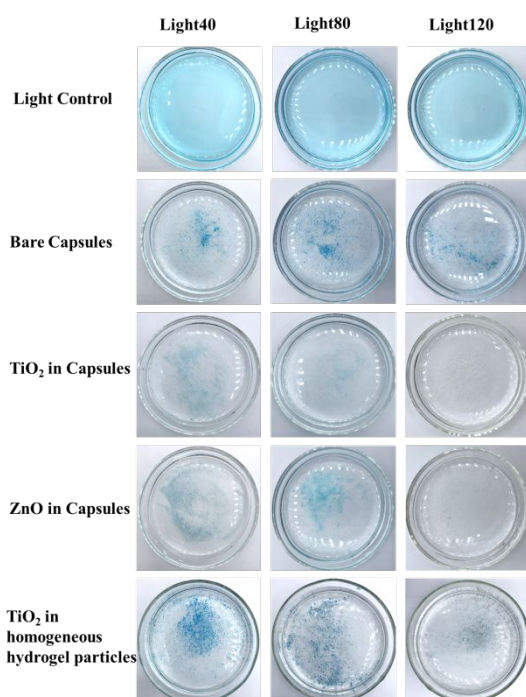

Figure 5. Optical images of microcapsules, PIC, and TiO$_2$ in HHP in MB aqueous after exposure to UV light (numbers represent time in minutes).

2.2.2 A removal of MB using flow microreactor

Flow microreactors based on the hydrogel capsules with aqueous photocatalytic core and permeable shells allow the construction of a new prototype device. Flow microreactors enable excellent control over reaction rates, diffusion, dynamic stirring of photocatalytic performance towards the direct adsorption, degradation and separation of pollutants. In our method, a large amount of PIC is loaded into the flash chromatographic column (17.0 mm outer diameter, 13.4 mm inner diameter) with a fritted glass bed and a

Teflon stopcock (**Figure 6a**). When the valve is opened, the MB solution flows through the filter consisting of the hydrogel microcapsules, while MB molecules are adsorbed by the PIC in the column. The 20 ml of MB solution are cleaned within 97 seconds. The inset UV-vis spectrum in **Figure 6a** indicates that nearly 100% MB is adsorbed by the PIC sample. In addition, the PIC in the flow reactor can be regenerated by a continuous exposure to UV light. Optical images are recorded every 30 min during the UV-regeneration process over 4.5 hours, shown in **Figure 6b**. The colour of the PIC solution is initially intense blue and finally, it returns to their original colourless appearance (slightly brown from the optical images, which can be attributed to a tiny amount MB remained in PIC due to UV unexposed parts in flow reactor).
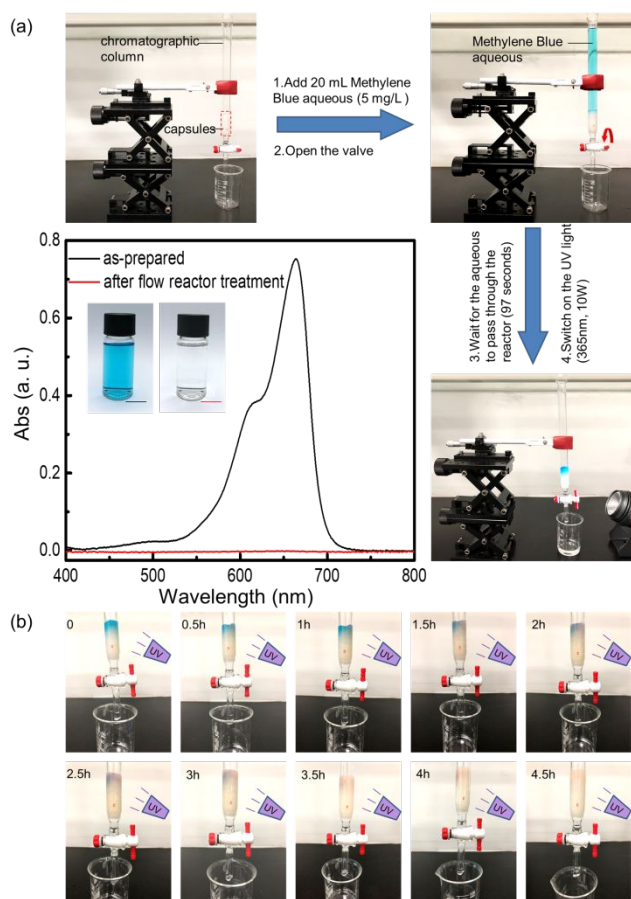
ARTICLE *Environmental Science: Nano*

Figure 6. Application of a prototype flow reactor combining direct solution flow for removal of MB contaminant. (a) Cleaning of MB solution by flowing it through the hydrogel microcapsule-based layers, while exposing photocatalytic core to UV light during 97 sec., (Inset a) UV-VIS spectrum of original and final MB solutions. (b) Photocatalytic regeneration process in the flow microreactor.

4. Conclusions

In summary, we demonstrate fabrication of poly(acid) hydrogel microcapsules containing photocatalytic nanoparticles in their aqueous core for the removal of MB pollutant. The synthesized PICs are characterized by FESEM, optical microscopy and FT-IR. Due to permeability of the hydrogel shell and its adsorptive performance, MB molecules can diffuse into the aqueous core of PIC, while ZnO and TiO$_2$ photocatalytic NPs stay trapped inside the functional core. A flow reactor device is designed to demonstrate the capabilities of a hydrogel capsule-filter, adsorbing nearly 100 % of MB over short time. Afterwards, the PIC materials are regenerated using UV light. Hydrogel capsules can potentially trap high surface area photo-catalytic nanomaterials as a liquid dispersion within the dynamic absorbent materials that can be easily removed from the environment unlike free photocatalytic nanoparticles. In this study, hydrogel capsules containing liquid photocatalytic core remove MB at rates comparable to photocatalyst enclosed in homogeneous hydrogel particles. Time of molecules/particles mixing in a fluidic volume can be estimated by the following equation $t_{mix} = d_c^2/D$, where d_c is the diameter of the capsule and D is the diffusion coefficient. Using traffic time one can also estimate how often

molecules/particles can meet in a fluidic volume $t_{traffic} = d_c^3/Dr$, where r is the sum of molecule/particle diameters.[69] As a result, a reduction of the diffusion constant in homogeneous hydrogels can increase time required for a pollutant adsorption/degradation. Consideration of typical mixing and traffic time in capsules and particles can provide insight into future design of more efficient chemical microreactors for adsorption/degradation of pollutants. For instance, it is of high interest to test efficiency of pollutants removal using significantly smaller capsules and photocatalytic nanoparticles.

5. Experimental methods

5.1 Materials and chemicals

Methacrylic anhydride (MAAn), ethylene glycol dimethacrylate (EGDMA), and radical photoinitiator 2- hydroxyl-2-methylpropiophenone (Darocure 1173), were purchased from Aladdin Industrial Corporation (USA). Sodium dodecyl benzene sulfonate (SDBS), poly (vinyl alcohol) (PVA, Mw 13000~23000), hydrogen peroxide, zinc oxide, potassium hydroxide and titanium oxide were provided by Hushi Corporation (China). Capillaries were provided by Jinglai Corporation (China). Microscope slides were purchased from Sail Brand (China). Epoxy adhesive were purchased from Ailete (China).

5.2 Microfluidic device preparation, synthesis of microcapsules and PIC

(1) Preparation of the glass capillary microfluidic device.

Two tapered cylindrical capillaries were obtained by fuse stretching (Capillary fuse stretcher (PC-10, NARISHIGE, Japan) and their tips were polished using sand paper to the appropriate sizes. The injection capillary was treated with octadecyltrimethoxysilane to obtain hydrophobic property, and the collection capillary was treated with 2-(methoxy(polyethyleneoxy)propyl)trimenthoxysilane to obtain hydrophilic property and prevent the double emulsion drops from wetting on the collection capillary wall. Capillaries were aligned inside of the square capillary (inner dimension: 1.05mm×1.05mm) whose inner dimensions were larger than the outer diameter of the tapered capillaries. Capillaries were fixed with 5-minute epoxy adhesive.

(2) Preparation of solutions

Outer phase (water+ PVA): 2 wt % PVA aqueous. Inner phase (water+ PVA+ photocatalysts): prepared by mixing 0.01g ZnO or TiO$_2$ in 10mL 2 wt % PVA aqueous, followed by the stirring the solutions for 6 hours.

Middle phase (monomers): the monomer mixture of EGDMA (5 mol % EGDMA) and MAAn (95 mol %) is degassed and 1 mol % Darocure 1173 is added before use.

(3) Microfluidic device assisted PIC preparation

As shown in **Figure 1 a** and **Figure 1b**, the outer phase, the inner phase, and the middle phase are injected into the corresponding inlets, and the double emulsion drops with monodisperse diameters are formed between the tapered inlet capillary tip and the outlet capillary tip (shown in **Figure 1 a** and **Figure 1c**). The drops are exposed to UV light (365nm, 10W) (AC80V-240V, Zhongshan Zigu Lighting Appliance Factory, China). After that, the capsules are immersed in pH=11 KOH solution for 1 day to be hydrolysed. The obtained samples are collected and washed with deionized water.

5.3 Characterizations

The morphologies of the microcapsules, PIC and Janus Pt/Fe/PIC were characterized by an optical microscope (BX51, Olympus Corporation, Japan) and a field emission scanning electron microscope (FESEM) (Sigma, Zeiss, Germany) at an accelerating voltage of 3 kV. To confirm the hydrolysis of the samples, the particles and particles were analysed by a Fourier transform infrared spectrometer (FT-IR) (Nicolet 6700, ThermoFisher, USA) after drying in vacuum. WAXS profiles were obtained at the beamline BL14B1-XRD of Shanghai Synchronization Radiation Facility (SSRF). The wavelength was 0.1214 nm, the end station was equipped with a Huber5021 diffractometer, and the sample to detector the distance 240 mm was calibrated by lanthanum boride (LaB).

5.4 MB removal studies

MB was employed as an organic dye contaminate to estimate the adsorptive performance and photocatalytic activity of the synthesized samples. For each experiment, 10 mL (5 mg/ L) MB solution was added into a quartz test tube and 0.05g samples was mixed in the solution. The dark reaction was conducted at room temperature under a gentle stirring. The light reaction was conducted under a 10 W UV lamp (365nm, 10W) (AC80V-240V, Zhongshan Zigu Lighting Appliance Factory, China) with a gentle stirring with a measured power density of 30 mW/cm². The MB concentration of every solution was measured by a UV-vis absorption spectrometer (UV-2550, Shimadzu Scientific Instruments, Japan) at intervals of 20 min. The following formula was used to calculate the removal efficiency (η) for CR:

$\eta = (C_0-C)/C_0$

(1)

where η is removal efficiency, C_0 and C are the initial MB concentration and the concentration of MB extracted within interval time, respectively.

A flow reactor was designed by filling the PIC in a flash chromatographic column. 20 mL (5 mg/ L) MB solution was treated by the prepared flow reactor, the concentration before and after the treatment was measured by a UV-vis absorption spectrometer. After that, the flow reactor was exposed to a 10 W UV lamp to regenerate the PIC, and its picture was recorded by a camera (iPhone 8) every 0.5 h.

Conflicts of interest

There are no conflicts to declare.

Acknowledgements

Notes and references

1   O. M. Rodriguez-Narvaez, J. Manuel Peralta-Hernandez, A. Goonetilleke and E. R. Bandala,   Treatment technologies for emerging contaminants in water: A review., *Chem. Eng. J.,* 2017, **323** , 361–380.
2   H. Hana, M. Khalid Rafiq, T. Zhoua, R. Xua, O. Mašek and X. Li. A critical review of clay-based composites with enhanced adsorption performance for metal and organic pollutants. *J. Hazard. Mater.*, 2019, **369**, 780–796.
3   X. L. Zhao, Y. C. Su, S. B. Li, Y. J. Bi and X. J. Han, A green method to synthesize flowerlike Fe(OH)$_3$ microspheres for enhanced adsorption performance toward organic and heavy metal pollutants, *J. Environ. Sci.*, 2018, 73, 45-57.
4   N. N. Wang, T. Zheng, G. S. Zhang and P. Wang, A review on Fenton-like processes for organic wastewater treatment, *J. Environ. Chem. Eng.*, 2016, **4**, 762-787
5   S. Thakur, P. P. Govender, M. A. Mamo, S. Tamulevicius and V. K. Thakur. Recent progress in gelatin hydrogel nanocomposites for water purification and beyond, *Vacuum*, 2017, **146**, 396-408.
6   S. Y. Lee and S. J. Park, TiO$_2$ photocatalyst for water treatment applications, *J. Ind. Eng. Chem.*, 2013, **19**(6), 1761-1769.
7   E. L. Cates, Photocatalytic Water Treatment: So Where Are We Going with This? , *Environ. Sci. Technol.*, 2017, **51**, 757-758.
8   A. Fujishima and K. Honda, Electrochemical Photolysis of Water at a Semiconductor Electrode, *Nature*, 1972, 238, 37-38.
9   S. Sakthivel, B. Neppolian, M. V. Shankar, B. Arabindoo, M. Palanichamy and V. Murugesan, Solar photocatalytic degradation of azo dye: comparison of photocatalytic efficiency of ZnO and TiO$_2$, *Sol. Energy Mater. Sol. Cells*, 2003, **77**, 65-82.
10 C. S. Turchi and D. F. Ollis, Photocatalytic degradation of organic- water contaminants mechanisms involving hydroxyl radical attack, *J. Catal.*, 1990, **122**, 178-192.
11 G. Odling and N. Robertson. Bridging the gap between laboratory and application in photocatalytic water purification, *Catal. Sci. Technol.*, 2019, **9**, 533-545.
12 K. Hashimoto and A. Fujishina. TiO$_2$ photocatalysis: A historical overview and future prospects, *Jpn. J. Appl. Phys.*, 2005, **44**, 8269-8285.
13 S. Kuriakose, N. Bhardwaj, J. Singh, B. Satpati and S. Mohapatra. Structural, optical and photocatalytic properties

of flower-like ZnO nanostructures prepared by a facile wet chemical method, *Beilstein J. Nanotechnol.*, 2013, **4**, 763-770.

14 K. He, G. Q. Chen, G. M. Zeng, A. W. Chen, Z. Z. Huang, J. B. Shi, T. T. Huang, M. Peng and L. Hu, Three-dimensional graphene supported catalysts for organic dyes degradation, *Appl. Catal., B*, 2018, **228**, 19-28.

15 D. Kim, R. Amos, M. Gauthier and J. Duhamel, Microfluidic Fabrication of Multistimuli-Responsive Tubular Hydrogels for Cellular Scaffolds, *Langmuir*, 2018, **34**, 8611-8621.

16 Y. H. La, B. D. McCloskey, R. Sooriyakumaran, A. Vora, B. Freeman, M. Nassar, J. Hedrick, A. Nelson and R. Allen. Bifunctional hydrogel coatings for water purification membranes: Improved fouling resistance and antimicrobial activity. *J. Membrane Sci.* **2011**, 372, 285-291.

17 J. K. Wychowaniec, M. Iliut, M. Zhou, J. Moffat, M. A. Elsawy, W. A. Pinheiro, J. A. Hoyland, A. F. Miller, A. Vijayaraghavan and A. Saiani, Designing Peptide/Graphene Hybrid Hydrogels through Fine-Tuning of Molecular Interactions, Biomacromolecules, 2018, **19**, 2731-2741.

18 M. Khan and IMC. Lo, A holistic review of hydrogel applications in the adsorptive removal of aqueous pollutants: Recent progress, challenges, and perspectives, *Water Res.*, 2016, **106**, 259-271.

19 I. N. Savina, G. C. Ingavle, A. B. Cundy and S. V. Mikhalovsky. A simple method for the production of large volume 3D macroporous hydrogels for advanced biotechnological, medical and environmental applications, *Sci. Rep.*, 2016, **6**, 21154-21162.

20 V. V. Tran, D. Park and Y. C. Lee, Hydrogel applications for adsorption of contaminants in water and wastewater treatment, *Environ. Sci. Pollut. Res.*, 2018, **25**, 24569-24599.

21 K. H. Yu, D. Wang and Q. M. Wang, Tough and Self-Healable Nanocomposite Hydrogels for Repeatable Water Treatment, *Polymers*, 2018, **10**, 880-891.

22 G. H. Jing, L. Wang, H. J. Yu, W. A. Amer and L. Zhang, Recent progress on study of hybrid hydrogels for water treatment, *Colloids Surf., A*, 2013, **416**, 86-94.

23 N. Pandey, S. K. Shukla and N. B. Singh, Water purification by polymer nanocomposites: an overview. *Nanocomposites,* 2017, **3**, 47-66.

24 L. Y. Sun, J. Wang, Y. R. Yu, F. K. Bian, M. H. Zou and Y. J. Zhao, Graphene oxide hydrogel particles from microfluidics for oil decontamination, *J. Colloid Interface Sci.*, 2018, **528**, 372-378.

25 R. Zowada and R. Foudazi, Porous Hydrogels Embedded with Hydrated Ferric Oxide Nanoparticles for Arsenate Removal, *ACS Appl. Polym. Mater.*, 2019, **1**, 1006-1014.

26 S. Basak, N. Nandi, S. Paul, I. W. Hamley and A. Banerjee, A tripeptide-based self-shrinking hydrogel for waste-water treatment: removal of toxic organic dyes and lead (Pb^{2+}) ions, *Chem. Commun.*, 2017, **53**, 5910-5913.

27 M. Y. Piao, D. L. Zou, Y. S. Yang, X. H. Ren, C. Y. Qin and Y. X. Piao, Multi-Functional Laccase Immobilized Hydrogel Microparticles for Efficient Removal of Bisphenol A, *Materials*, 2019, **12**, 704-717.

28 Y. H. Guo, X. Y. Zhou, F. Zhao, J. Bae, B. Rosenberger and G. H. Yu, Synergistic Energy Nanoconfinement and Water Activation in Hydrogels for Efficient Solar Water Desalination, *ACS Nano*, 2019, **13**, 7913-7919.

29 X. Y. Zhou, F. Zhao, Y. H. Guo, B. Rosenberger and G. H. Yu. Architecting highly hydratable polymer networks to tune the water state for solar water purification, *Sci. Adv.*, 2019, **5**, eaaw5484.

30 M. Khan and I. M. C. Lo, Removal of ionizable aromatic pollutants from contaminated water using nano gamma-Fe_2O_3 based magnetic cationic hydrogel: Sorptive performance, magnetic separation and reusability, *J. Hazard. Mater.*, 2017, **322**, 195-204.

31 F. Zhao, X. Y. Zhou, Y. Shi, X. Qian, M. Alexander, X.P. Zhao, S. Mendez, R. G. Yang, L.T. Qu and G. H. Yu, Highly efficient solar vapour generation via hierarchically nanostructured gels, *Nat. Nanotechnol.*, 2018, **13**, 489-495.

32 D. Li, X. Y. Zhang, G. P. Simon and H. T. Wang, Forward osmosis desalination using polymer hydrogels as a draw agent: Influence of draw agent, feed solution and membrane on process performance, 2013, **47**, 209-215.

33 W. Ali, B, Gebert, S. Altinpinar, T. Mayer-Gall, M. Ulbricht, J. S. Gutmann and K. Graf, On the Potential of Using Dual-Function Hydrogels for Brackish Water Desalination, Polymer, 2018, **10**, 567.

34 H. Lu, S. T. Zhang, L. Guo and W. H. Li, Applications of graphene-based composite hydrogels: a review, *RSC Adv.*, 2017, **7**, 51008-51020.

35 M. Khan and I. M. C. Lo, A holistic review of hydrogel applications in the adsorptive removal of aqueous pollutants: Recent progress, challenges, and perspectives, *Water Res.,* 2016, **106**, 259-271.

36 H. Ning, Y. Zhang, H. Zhu, A. Ingham, G. S. Huang, Y. F. Mei and A. A. Solovev, Geometry design, principles and assembly of micromotors, *Micromachines*, 2018, **9**, 75

37 F. Z. Mou, D. Pan, C. R. Chen, Y. R. Gao, L. L. Xu and J. G. Guan, Magnetically Modulated Pot-Like $MnFe_2O_4$ Micromotors: Nanoparticle Assembly Fabrication and their Capability for Direct Oil Removal, *Adv. Funct. Mater.*, 2015, **25**, 6173-6181.

38 Q. L. Zhang, R. F. Dong, Y. F. Wu, W. Gao, Z. H. He and B. Y. Ren, Light-Driven $Au-WO_3$@C Janus Micromotors for Rapid Photodegradation of Dye Pollutants, *ACS Appl. Mater. Interfaces*, 2017, **9**, 4674-4683.

39 S. Wang, Z. Z. Jiang, S. S. Ouyang, Z. P. Dai and T. Wang. Internally/Externally Bubble-Propelled Photocatalytic Tubular Nanomotors for Efficient Water Cleaning, *ACS Appl. Mater. Interfaces*, 2017, **9**, 23974-23982.

40 M. Safdar, J. Simmchen and J. Janis, Light-driven micro- and nanomotors for environmental remediation, *Environ. Sci.: Nano*, 2017, **4**, 1602-1616.

41 Z. J. Zhang, A. D. Zhao, F. M. Wang, J. S. Ren and X. G. Qu, Design of a plasmonic micromotor for enhanced photo-remediation of polluted anaerobic stagnant waters, *Chem. Commun.*, 2016, **52**, 5550-5553.

42 J. X. Li, V. V. Singh, S. Sattayasamitsathi , J. Orozco, K. Kaufmaan, R. F. Dong, W. Gao, B. Jurado-Sanchez, Y. Fedorak and J. Wang, Water-Driven Micromotors for Rapid Photocatalytic Degradation of Biological and Chemical Warfare Agents, *ACS Nano*, 2014, **8**, 11118-11125.

43 W. Gao and J. Wang, The Environmental Impact of Micro/Nanomachines: A Review, *ACS Nano*,2014, **8**, 3170-3180.

44 B. Jurado-Sanchez and W. Joseph, Micromotors for Environmental applications: a review, *Environ. Sci.: Nano*, 2018, **5**, 1530-1544.

45 S. K. Srivastava, M. Guix and O. G. Schmidt, Wastewater Mediated Activation of Micromotors for Efficient Water Cleaning, *Nano Lett.*, 2016, **16**, 817-821.

46 A. Q. Chen, X. H. Ge, J. Chen, L. Y. Zhang and J. H. Xu, Multi-functional micromotor: microfluidic fabrication and water treatment application, *Lab Chip*, 2017, **17**, 4220-4224.

47 L. Soler and S. Sanchez, Catalytic nanomotors for environmental monitoring and water remediation, *Nanoscale*, 2014, 6, 7175-7182.

48 Z. H. Lin, Z. G. Wu, X. K. Lin and Q. He, Catalytic Polymer Multilayer Shell Motors for Separation of Organics, *Chem. - Eur. J.*, 2016, **22**, 1587-1591.

49 M. Safdar, S. U. Khan and J. Janis, Progress toward Catalytic Micro- and Nanomotors for Biomedical and Environmental Applications, *Chem. - Eur. J.*, 2018, **30**, 1703660.

50 J. Parmar, D. Vilela, K. Villa, J. Wang and S. Sanchez, Micro- and Nanomotors as Active Environmental Microcleaners and Sensors, *J. Am. Chem. Soc.*, 2018, **140**, 9317-9331.

51 C. Y. Liang, C. Zhan, F. Y. Zeng, D. D. Xu, Y. Wang, W. W. Zhao, J. H. Zhang, J. H. Guo, H. H. Feng and X. Ma, Bilayer Tubular Micromotors for Simultaneous Environmental Monitoring and Remediation, *ACS Appl. Mater. Interfaces*, 2018, **10**, 35099-35107.

52 S. Naeem, F. Naeem, M. Manjare, F. Liao, V. A. Bolaños Quiñones, G. S. Huang, Y. Li, J. Zhang, A. A. Solovev, Y. F. Mei, Tubular catalytic micromotors in transition from unidirectional bubble sequences to more complex bidirectional motion, *Appl. Phys. Lett.*, 2019, **114**, 033701.

53 Y. L. Ying and M. Pumera, Micro/Nanomotors for Water Purification, *Chem. - Eur. J.*, 2019, **25**, 106-121.

54 W. Gao, X. M. Feng, A. Pei, Y. E. Gu, J. X. Li and J. Wang, Seawater-driven magnesium based Janus micromotors for environmental remediation, Nanoscale, **5**, 4696-4700.

55 H. He, R. Buchel, R. Figi, Y. C. Zhang, U. Bahk, J. Ma, and J. Wang, High-performance carbon/MnO_2 micromotors and their applications for pollutant removal, *Chemosphere*, 2019, **219**, 427-435.

56 W. J. Liu, H. B. Ge, X. Chen, X. L. Lu, Z. W. Gu, J. X. Li and J. Wang, Fish-scale-like intercalated Metal Oxide-Based Micromotors as Efficient Water Remediation Agents, *ACS Appl. Mater. Interfaces*, 2019, **11**, 16164-16173.

57 H. Wang, X. Y. Gu and C. Y. Wang, Self-Propelling Hydrogel/Emulsion-Hydrogel Soft Motors for Water Purification, *ACS Appl. Mater. Interfaces*, 2016, **8**, 9413-9422.

58 R. Q. Wang, W. L. Guo, X. H. Li, Z. H. Liu, H. Liu and S. Y. Ding, Highly efficient MOF-based self-propelled micromotors for water purification, *RSC Adv.*, 2017, **7**, 42462-42467.

59 H. Wang, B. Khezri and M. Pumera. Catalytic DNA-Functionalized Self-Propelled Micromachines for Environmental Remediation, *Chem*, 2016, **1**, 473-481.

60 B. Jurado-Sanchez, S. Sattayasamitsathit, W. Gao, L. Santos, Y. Fedorak, V. V. Singh, J. Orozco, M. Galarnyk, and J. Wang. Self-Propelled Activated Carbon Janus Micromotors for Efficient Water Purification, *Small*, **11**, 499-506.

61 D. Vilela, J. Parmar, Y. F. Zeng, Y. L. Zhao and S. Samuel, Graphene-Based Microbots for Toxic Heavy Metal Removal and Recovery from Water, *Nano Lett.*, 2016, **16**, 2860-2866.

62 X. He, Y. K. Bahk and J. Wang, Organic dye removal by MnO2 and Ag micromotors under various ambient conditions: The comparison between two abatement mechanisms, *Chemosphere*, 2017, **184**, 601-608.

63 V. V. Singh, B. Jurado-Sanchez, S. Sattayasamitsathit, J. Orozco, J. X. Li, M. Galarnyk, Y. Fedorak and J. Wang. Multifunctional Silver-Exchanged Zeolite Micromotors for Catalytic Detoxification of Chemical and Biological Threats. *Adv. Funct. Mater.*, 2015, **25**, 2147-2155.

64 C. R. Chen, E. Karshalev, J. G. Guan and J. Wang, Magnesium-Based Micromotors: Water-Powered Propulsion, Multifunctionality, and Biomedical and Environmental Applications, *Small*, 2018, **14**, 1704252.

65 H. Eskandarloo, A. Kierulf and A. Abbaspourrad, Nano- and micromotors for cleaning polluted waters: focused review on pollutant removal mechanisms, *Nanoscale*, 2017, **9**, 13850-13863.

66 L. L. Zhang, Y. L. Nie, C. Hu and X. X. Hu, Decolorization of methylene blue in layered manganese oxide suspension with H_2O_2, *J. Hazard. Mater.*, 2011, **190**, 780-785.

67 J. G. Werner, S. Nawar, A. A. Solovev, D. A. Weitz, Hydrogel Microcapsules with Dynamic pH-Responsive Properties from Methacrylic Anhydride, *Macromolecules*, 2018, **51**, 5798-5805.

68 J. G. Werner, B. T. Deveney, S. Nawar and D. A. Weitz, Dynamic Microcapsules with Rapid and Reversible Permeability Switching, *Adv. Funct. Mater.*, 2018, 28, 1803385.

69 H. Zhu, S. Nawar, J. G. Werner, J. R. Liu, G. S. Huang, Y. F. Mei, D. A. Weitz and A. A. Solovev, Hydrogel micromotors with catalyst-containing liquid core and shell, *J. Phys.: Condens. Matter*, 2019, **31**, 214004.

70 A. Moncho-Jorda, A. German-Bellod, S. Angioletti-Uberti, I. Adroher-Benitez and J. Dzubiella, Nonequilibrium Uptake Kinetics of Molecular Cargo into Hollow Hydrogels Tuned by Electrosteric Interactions, *ACS Nano*, 2019, **13**, 1603-1616.

71 R. Dembczynski and T. Jankowski, Characterisation of small molecules diffusion in hydrogel-membrane liquid-core capsules, *Biochem. Eng. J.*, 2000, **6**, 41-44.

72 B. Amsden, Solute Diffusion within hydrogels. Mechanisms and models, *Macromolecules*, 1998, **31**, 8382-8395.

73 B. Amsden, Solute diffusion in hydrogels. An examination of the retardation effect, *Polym. Gels Networks*, 1998, **6**, 13-43.

74 S. P. Zustiak, H. Boukari and J. B. Leach, Solute diffusion and interactions in cross-linked poly(ethylene glycol)hydrogels studied by fluorescence correlation spectroscopy, *Soft Matter*, 2010, **6**, 3609-3618.

1
2
3
4
5
6
7
8
9
10
11
12
13
14
15
16
17
18
19
20
21
22
23
24
25
26
27
28
29
30
31
32
33
34
35
36
37
38
39
40
41
42
43
44
45
46
47
48
49
50
51
52
53
54
55
56
57
58
59
60

Hydrogel Microcapsules with Photocatalytic Nanoparticles for Removal of Organic Pollutants

Jinrun Liu,[a] Chen Hong,[a] Xiaojie Shi,[a] Saraf Nawar,[b] Jörg G. Werner,[b] Gaoshan Huang,[a] Miaomiao Ye,[c] David A. Weitz[b‡] Alexander A. Solovev*[a] and Yongfeng Mei*[a]

Table of Contents Entry
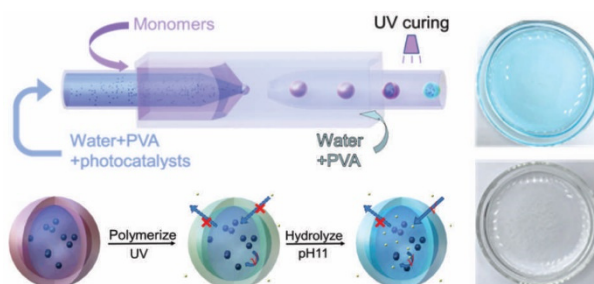
Droplet-based microfluidics is used to fabricate hydrogel microcapsules with water permeable shells and aqueous core containing encapsulated photocatalytic nanoparticles for the removal of methylene blue from aqueous solutions.